Computational Toxicology 13 (2020) 100113

Contents lists available at ScienceDirect

Computational Toxicology

journal homepage: www.elsevier.com/locate/comtox

Examining the *in vivo* pulmonary toxicity of engineered metal oxide nanomaterials using a genetic algorithm-based dose-response-recovery clustering model

Vignesh Ramchandran, Jeremy M. Gernand*

Department of Energy and Mineral Engineering, Pennsylvania State University, University Park, PA 16802, United States

ARTICLE INFO

Keywords:
Dose-response
Recovery
Pulmonary toxicity
Metal oxides
Hierarchical clustering
Potency

ABSTRACT

This article presents the examination of the pulmonary toxicity of engineered metal oxide nanoparticles using a dose-response-recovery clustering model for the purpose of revealing toxicologically distinct clusters. Current recommended exposure limits published by the National Institute for Occupational Safety and Health (NIOSH) consider "ultrafine" metal oxide particles to pose significantly increased health risks as compared to larger particles. The unique combination of physical and chemical characteristics afforded by the metal oxide nanoparticles has enabled them to find use in various large-scale industrial setting leading to a risk of exposure for current and future workers. This paper presents an algorithmic examination of the metal oxide nanoparticles by their categorization into toxicologically distinct clusters. Based on a dataset composed of peer-reviewed *in vivo* experimental studies in rodents, the metal oxide nanoparticle variants are divided into sub-classes based on their dose-response-recovery similarity and the Akaike Information Criterion (AIC) of the family of models. Results indicate the presence of 4 toxicologically unique classes based on 5 toxicity endpoints selected. The cluster with greatest potency was found to be 400,000 times more potent than the cluster with the lowest potency indicative of substantial variation across all the responses. The absence of coherent characterization data for the metal oxide nanoparticle variants analyzed in this study prevents the designation of significant physical characteristic-based labels which could have assisted in identifying the key factors affecting the toxic potential of the metal oxide nanoparticles. The standardized potency of the 4 metal oxide nanoparticle clusters was compared: 3 clusters (I, II and IV) showed signs of elevated immune system activity and cell membrane damage. These clusters were primarily composed of iron oxide nanoparticles (cluster I) silica (cluster II), and titanium dioxide (cluster IV). One cluster (III) showed comparatively reduced toxicity across all 5 responses; this cluster primarily featured zinc oxide and cerium oxide nanoparticles.

1. Introduction

Toxicological testing necessary for the establishment of safe exposure levels to emerging pollutants can be time consuming and resource intensive [1]. When the emerging pollutant is an engineered nanoparticle, whose chemical and physical nature can be changed at the will of the designer, the pace of development for new nanoparticle variants is too rapid for such safety testing to keep up. Some of these NMs might eventually prove to be a serious occupational hazard or become an environmental pollutant presenting risk to the people working with them and to those who use the technology or live near places they are used. Anticipating the toxicological impact and exposure response to newly synthesized nanoparticles is difficult. Metal oxide nanoparticles (MONP's) are particularly popular in industrial environments due to the diverse array of benefits offered by virtue of their small size. For example, ultrafine (< 100 nm) metal oxides such as aluminum oxide and cerium oxide are employed as fuel additives to lower emissions and promote more efficient combustion [2]. Similarly, nano-titanium dioxide is a popular component of multiple food, personal care, and consumer products [3]. Exposure to ultrafine particles induces both acute and chronic inflammatory response, nano-ceria has been known to disperse with diesel exhaust leading to potential pulmonary fibrosis [4,5]. Further evidence of pulmonary response exposure to ultrafine particles has been documented for various metal

Abbreviations: MONP, Metal oxide nanoparticles; BAL, bronchoalveolar lavage; MAC, macrophage count in BAL fluid; TP, total protein concentration in BAL fluid; LDH, lactose dehydrogenase; PMN, polymorphonuclear neutrophil; TC, total cell count

* Corresponding author.
E-mail address: jmgernand@psu.edu (J.M. Gernand).

https://doi.org/10.1016/j.comtox.2019.100113
Received 13 June 2019; Received in revised form 17 September 2019; Accepted 18 November 2019
Available online 27 November 2019

oxide particles [6–9]. NIOSH has set recommended exposure limits (REL) of 2400 μg/m^3 and 300 μg/m^3 for fine-sized (respirable) and ultrafine-sized titanium dioxide. A REL for respirable crystalline silica has also recently been revised 50 μg/m^3, but there is no current recommendation for ultrafine silica. It is yet unclear whether new RELs (and eventually associated regulatory limits based on the recommendations) will be set at similarly reduced levels for most other metal oxide nanoparticles or not. These limits are derived from the extrapolation of the effects of pulmonary exposure in Rats to Humans [10,11].

Experimental toxicology testing studies are often time consuming and require considerable investment with collective costs potentially running up to billions of dollars [12]. A study published in 2011 about the long term development of NMs projected that up to 6 million individuals could potentially be exposed by 2020 [13]. One potential solution to this problem is prioritizing the testing the NMs targeting the more toxic varieties first. The development of computational approaches targeted at predicting the toxicity of the NMs based on their attributes can be used as a means to guide nanomaterial synthesis towards less hazardous variants. Experimental evaluation is subject to a certain degree of error or bias and in some cases the results may be difficult to replicate. To overcome some of these inefficiencies, forecasting methods have been proposed to predict the potential toxicity and environmental impact of new NMs [14]. Computational modeling of nanotoxicity is valuable for its efficiency of time and expense and the flexibility offered. Quantitative structure activity relationships (QSARs) are one of the modeling schemes currently utilized; these models hypothesize that the activity of any nanostructure is a function of its physicochemical properties [15,16]. Puzyn et al. demonstrated the use of QSARs to predict the mechanism of cytotoxicity of 17 different metal oxide nanoparticles [14]. QSAR modeling and novel descriptors have previously used in conjunction to predict the cytotoxicity of metal oxide nanoparticles using E. coli exposure studies [17]. The cell viability of human lung and skin cells upon exposure to metal oxide nanomaterials has also been predicted using QSAR based modeling [18].

Meta-analysis is a useful analytical method for harnessing the available published nanotoxicology data, and testing hypotheses that were not possible within the original experiments. Meta-analyses employ statistical and/or machine learning approaches such as regression, neural networks, decision trees, and support vector machines to identify important associations [19]. Since meta-analysis curates data from multiple sources, the individual variation or appearance of unusual results across the complete dataset are evaluated in light of the whole. Traditional meta-analysis, which involves literature-based data collection, can in some cases be ineffective in this case due to the presence of missing data caused by disparity in NM characterization methods [20]. A meta-analysis published in 2013 on the health effects of exposure to nano-TiO_2 concluded that the particles were retained in several key organs in the body [21]. Meta-analysis has also been used to assess the toxicity of NMs when they are dissolved—a possibility with high-solubility metal oxide nanoparticles [22]. The prediction of carcinogenic potency using historical *in vivo* genotoxicity data has also been accomplished using meta-analysis [23]. The benefits of meta-analysis techniques include its ability to identify the sources of diversity across the various participating studies [24], it can be used to improve the precision of the estimates due to the increase in the size of the population [25]. The method however is not without its limitations: it has no control over the homogeneity of the participating studies [24]; it cannot improve the quality of the data used and consequently the final result; and it could suffer from "publication bias", where researchers fail to report or exclude certain studies to present a more coherent result which could impact the analysis [25].

Multiple researchers have documented the adverse effects associated with exposure to metal oxide nanoparticles. Peng et al (2014) compared the pulmonary toxicity of 2 types of nano-ceria and concluded that smaller agglomerates were more potent due to higher lung deposition [5]. Kadoya et al (2011) compared micro-sized and sub-micron sized nickel oxide and deduced that sub-micron sized particles induce stronger effects in the BAL fluid [26]. Titanium dioxide and silica have been extensively documented for their toxicological response with multiple researchers concluding that large doses of ultrafine Titania and silica induces immune response in subjects [6,7,9,27–36]. Similarly, articles documenting the effects of exposure to zinc, iron and other metal oxides have described the negatives effects associated with their exposure [8,37–42].

Attempts at using computational modeling to predict the effects on toxicity of changes in particle properties (QSARS, meta-analysis etc.) have been limited in their scope to date. These methods have either been exclusive to only metal oxide particles, particles of a particular size, cytotoxicity assays, or structural analysis of single particles [14,43–47]. There is a need to quickly identify and prioritize the testing of NMs which pose greater risk than others to maximize their benefit while simultaneously minimizing the risk associated with them. This could be accomplished by quantifying the current knowledge base of *in vivo* and *in vitro* studies to reveal how different NMs compare to one another and how changes in their properties affect their toxicity. The rapid increase in the number of synthesized NMs variants reveals a need to cluster the variants displaying similar effects as a means of generating hypotheses about the mechanisms of their pulmonary toxicity. To address the question of how different metal oxide nanomaterials can be considered the same substance toxicologically, this study proposes a new algorithmic approach applied to meta-analysis of extant metal oxide nanoparticle *in vivo* toxicity data.

2. Methods

2.1. 1 Data selection

The data utilized for the meta-analysis of the *in vivo* pulmonary toxicity of metal oxide nanoparticles is curated from 30 different peer-reviewed journal articles. These publications were identified through online search engines including the Web of Science, Google Scholar, and PubMed using the search terms: "*in vivo*", "Metal oxide", "BAL" and "Pulmonary". The publications are all independent "*in vivo*" studies conducted on metal oxide nanoparticles, they are a collection of exposure groups (experiments) identified by their total dosage, method of exposure (inhalation, instillation, aspiration etc.), post-exposure recovery period, and an independent characterization profile (physical and chemical properties) of the particles. The data extracted from the publications identified and included as part of the dataset additionally satisfied a key criterion before inclusion: the measures of response in Bronchoalveolar lavage (BAL) fluid for the rodents must be recorded for a minimum of 3 different levels (including the control level) of dose or exposure. All publications used as the source for this analysis have been provided in Table 1.

The five quantitative response measures from the BAL fluid which are the focus of this meta-analysis include: Total cell count (TCC), Macrophage count (MAC), Total protein concentration (TP), Polymorphonuclear neutrophil count (PMN) and Lactate dehydrogenase concentration (LDH). These 5 measures were reported in sufficient capacity across the publications to be included in this analysis. The measured response reported in each publication is expressed as a fold (multiple) of its respective control group's measure.

2.2. Model definition

The dose-response model used for the clustering analysis is an important feature of the process; it reflects the variation of the response to changes in the applied dose. Benchmarked dose-response models have been previously developed to analyze the response to multiple engineered substances. Slob (2001) has previously published a family of 3-parameter models available for analyzing continuous data, but these

Table 1
Compilation of the data (with sources) used for the MONP clustering process. (NR designation indicates "Not Reported").

SourceID	Primary Author	MONP Types Tested	No. of endpoints (of interest) reported	Total No. of exposure groups	MONP Typical Size (nm)	Average Specific Surface Area (m^2/g)
T1	Nemmar [54]	Titanium	2	3	4–6	49.4
T2	Oberdorster [29]	Titanium	4	7	20–250	NR
T3, S1	Warheit [55]	Titanium, Silica	4	36	5.8 – 6.1 (T3), 1500 (S1)	51.5
T4	Renwick [56]	Titanium	4	6	29–250	28.2
T5, S2	Rehn [57]	Titanium, Silica	4	30	20 (T5), 900 (S2)	NR
T6	Grassian [32]	Titanium	3	16	3.5 – 17.8	130
T7, S3	Warheit [58]	Titanium, Silica	4	88	25 (T7), 200 – 2000 (S3)	23.6
T8, S4	Warheit [35]	Titanium, Silica	3	20	100 (T8), 534 (S4)	26.4
T9, S5	Kobayashi [59]	Titanium, Silica	3	41	4.9 – 154.2	233.6
T10, T13	Gustafsson [6]	Titanium	3	16	21	NR
T11	Oyabu [28]	Titanium	3	20	14	102
T12	Roberts [60]	Titanium	3	12	21.75	NR
T14	Silva [9]	Titanium	1	14	24–28	113
S6	Gosens [61]	Silica	4	4	NR	NR
S7	Cho [62]	Silica	4	16	14	NR
S8	Creutzenberg [31]	Silica	5	6	76	21.2
S9	Roursgaard [34]	Silica	3	21	100–1600	20.7
N7	Morimoto [63]	Nickel	2	5	20	NR
F1	Ban [37]	Iron	2	11	35–147	22.5
F2	Pirela [64]	Iron	4	4	19.6	41.5
F3	Zhu [40]	Iron	4	13	22–280	28.8
F4	Katsnelson [39]	Iron	3	4	10–1000	NR
S10, Z1	Sayes [30]	Silica, Zinc	3	36	90–452	26.1
Ce1	Toya [65]	Cerium	4	17	200–3900	NR
N1	Morimoto [66]	Nickel	1	15	20	104.6
Z2, F5	Xia [42]	Zinc, Iron	2	15	8 – 20.2	97.5
S11, Z3	Warheit [36]	Silica, Zinc	3	28	90 – 111 (Z3)	10.9
T15, S12, Ce2, Z4, N2, Cu1	Cho [7]	Titanium, Silica, Cerium, Zinc, Nickel, Copper	3	24	10–35	93.7
Ce3	Ma [67]	Cerium	3	18	20	NR
Ce4	Peng [5]	Cerium	4	12	4	NR
T16, S13	Roursgaard [27]	Titanium, Silica	3	28	8–1600	112
T17, S14, A1	Lindenschmidt [33]	Titanium, Silica, Aluminum	5	45	2200–5300	NR
Ce5	Park [68]	Cerium	3	7	NR	NR
Ce6	Wingard [69]	Cerium	3	4	8	44
Ce7	Xue [70]	Cerium	3	15	6.6	86.8
Ce8	Ma [4]	Cerium	2	6	10.14	90
Ce9	Minarchick [71]	Cerium	2	4	4	81.4
T18, Co1	Dick [72]	Titanium, Cobalt	3	6	20	43.4
S15, M1	Gelli [41]	Silica, Magnesium	1	15	50–63000	22.5 (M1)
T19, S16, Co2	Zhang [73]	Titanium, Silica, Cobalt	5	25	20–1850	45.6
T20, N3	Horie [74]	Titanium, Nickel	2	16	7–1000	NR
T21, S17, N4	Kadoya [26]	Titanium, Silica, Nickel	1	25	27–2700	16.5
T22, S18, N5	Ogami [75]	Titanium, Silica, Nickel	2	25	27–2700	16.5
N6, Z5, Cu2	Cho [38]	Nickel, Zinc, Copper	2	8	10–50	56.3
Z6	Cho [8]	Zinc	4	9	10.7	48.2
N8	Nishi [76]	Nickel	2	15	20	NR

models do not reflect the variation in the measured response when exposure has ceased, and the test subject has begun to recover. This paper proposes a revision to one of Slob's model, the addition of a fourth parameter that describes the decrease of the response measure over time (i.e. the animal recovers) to provide a more complete description of the dose-response-recovery relationship. The relation between the response measured (y), dosage applied (x) and post-exposure recovery period (t) is,

$$y = a[c - (c - 1)e^{-bx}] - dt \quad (1)$$

The 4 parameters, a (signifies the response at dose = 0), b (the toxic potency of the nanoparticles), c (the maximum relative shift in response), and d (slope of the response decay) are the key parameters which have been used to describe the potential of the particle to be a hazard.

Recovery is likely to have an exponential relationship as the animal returns to homeostasis following the end of exposure. However, since such a relationship would require the addition of two additional model parameters, rather than one for the linear term, and given the available data fit the linear representation of recovery better, we make the parsimonious choice here with the single caveat that the model is valid for all recovery times, t, until the value of the response returns to 1 (i.e. no change from the control group).

2.3. Clustering algorithm

The proposed algorithm is aimed at assigning the metal oxide nanoparticles into "clusters" based on the similarity of their dose-response-recovery relationships. The methodology is a derivation of the traditional top-down hierarchical clustering process and mimics its structure. The algorithm utilizes non-linear regression to fit the proposed dose-response-recovery model (Eq. (1)) to the available data. The process involves using an exhaustive search approach driven by combinatorics to identify the ideal number of cluster constituents at each stage. A detailed explanation of the entire clustering process has been covered in a previous article by the authors and can be referenced for further clarity on the process [48].

The clustering approach yields multiple possibilities in terms of the

total number of clusters and the membership within those clusters which are assessed using a performance metric to avoid overfitted solutions. The performance metric used here to evaluate the goodness of a cluster is the Akaike Information Criterion (AIC), the AIC is calculated based on the number of parameters (k) in a model and its log-likelihood (L),

$$AIC = 2k - 2\log L \tag{2}$$

The likelihood function of a model is defined as the probability of that model achieving an outcome given a set of parameters, maximizing the likelihood function reduces the error between the expected and observed data. We assume the likelihood function of the model follows a normal distribution and its logarithmic form represented mathematically as,

$$logL(\mu, \sigma) = -n\log(\sigma) - \frac{n}{2}log(2\pi) - \frac{1}{2\sigma^2}\sum_{1}^{n}(Y_i - \mu)^2 \tag{3}$$

Y_i, represents the model derived response data, μ and σ represent the mean of the experimentally measured response and its associated standard deviation, n represents the number of exposure groups present in the model.

The overall AIC of a cluster is obtained by summing together the AIC values of its component models. Lower values of AIC are preferred when comparing the clusters as they indicate the model is closer to the data in those cases. AIC needs to be modified to include corrections that can be applied when dealing with small datasets, this corrected form is denoted as the AICc.

$$AICc = AIC + \frac{2k(k+1)}{n-k-1} \tag{4}$$

where n is the number of observations and k is the number of model parameters. The AICc is the best metric for comparing the amount of information conveyed by distinct models of varying complexity or as in our case comparing multiple cluster configurations [49]. We adopt the AICc as our measure of performance since it issues a strong penalty to those clusters where there is evidence of overfitting.

2.4. Genetic algorithm

An exhaustive clustering algorithm would be inefficient when deployed on large datasets. The current size and presumably the future increasing availability of data for the metal oxide nanoparticle response measures would result in high computational time requirements. Fig. 1 shows the steep increase in the total number of cluster configurations analyzed as the number of particles expands.

The search space for the metal oxide dataset has a large number of possible configurations (order of magnitude: 10^{10}), given the variety of unique nanoparticles included, employing an exhaustive search algorithm on this dataset yielded unrealistic completion times. An alternative approach to search the available space to identify the solution is to use Genetic algorithms (GA). Genetic algorithms use an adaptive and heuristic approach towards determining the solution to a search problem, the underlying principle to their methodology is the process of natural selection which is the driving factor behind biological evolution.

The original clustering algorithm has been incorporated within a genetic algorithm framework which facilities identification of the ideal cluster constituents from the large search space. Each stage of the clustering process is subjected through a genetic algorithm to identify the ideal dissociation of the data into clusters. The AICc score of the clusters are used to compare and select the best cluster combination for the complete data. The objective function minimized by the algorithm can be mathematically expressed as,

$$Y = \sum_{i=1}^{n} AIC_i \tag{5}$$

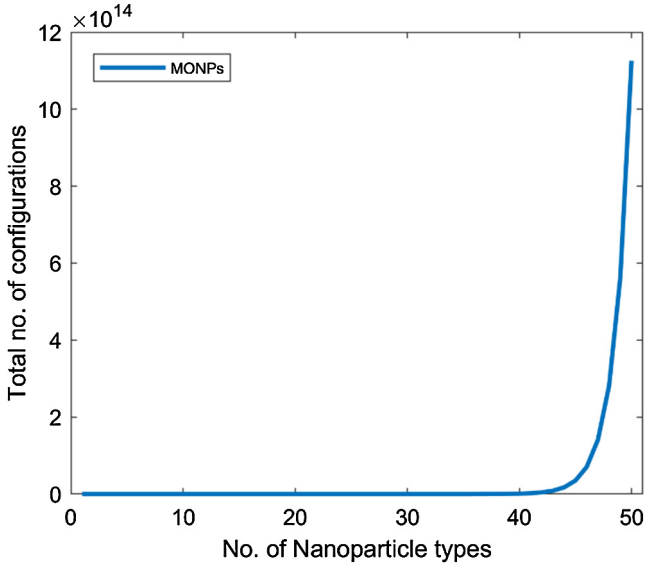

Fig. 1. Variation between the total number of cluster membership configurations analyzed vs the number of unique nanoparticle types. The plot demonstrates the increasing computational load as more particles are added to the analysis.

where, Y represents the overall AIC score of the clusters used to represent the data, the individual cluster AIC is computed using Eq. (2) referenced earlier, n is the number of clusters at each stage of the evaluation.

For example, if the dataset were to contain 35 particle variants, the next step in the process would determine using combinatorics the multiple possible ways to separate the 35 particle variants into 2 clusters, but each of those has multiple scenarios. Assume for illustration a cluster of 1 particle and a second containing 34 particles expressed as (134) can be accomplished in 35 ($^{35}C_1$) unique ways, while a (233) split has 595 ($^{35}C_2$) unique groupings and so on. These are just a few of the "configurations" available when deciding which is the ideal grouping possible, an exhaustive search through all the possibilities is time consuming.

The GA was implemented using MATLAB R2017b [50]. The algorithm uses a "Bit String" population input i.e. the "genes" in the algorithm correspond to various particle variants encoded as 0 or 1, and the "chromosomes" that compose the population are all the possible solutions to the optimization problem. The mutation and crossover functions for the GA are set to be "Uniform" with a 1% rate of mutation (uniform and random gene replacement throughout the progression) and "Scattered" (randomized crossover points to generate new chromosomes) respectively. The new "generations" (population of every iteration) are synthesized from the parent chromosomes using an 80% rate of crossover. The stopping criteria for the algorithm is set at 100 "Stall Generations" (i.e. when the best solution does not change for 100 generations as computed by the algorithm).

One limitation of the GA is the possibility of identifying a local solution to the AICc minimization problem rather than the global solution. There are testing methods to significantly reduce the possibility of this result. Multiple iterations of the overall GA process could be conducted, and a statistical distribution could be generated of the derived results, the alternative would be to compare the results of the GA with the results of a brute force algorithmic search. The results from the brute force algorithm would align with the global solution due to the rigorous nature of the search mechanism.

An alternative to the GA is another stochastic search method known as Simulated Annealing. Simulated annealing is an approach to solving optimization problems such as this one: the identification of similar toxicological groups with the minimum AIC. However, given the

specifics of this problem including the very large sample space and the need to employ parallel processing, simulated annealing was not anticipated to provide any meaningful benefits in terms of processing time or the fitness of the identified solutions. Several other studies have come to similar conclusions under similar circumstances [18,49,51–53].

3. Results and discussion

3.1. Composition-blind clustering results

The clustering analysis was conducted on the Metal Oxide Nanoparticles (MONP) dataset. The dataset for the MONP's contains several studies where more than 1 unique set of nanoparticles is analyzed. These studies were identified and separated to ensure each study reflects a single particle i.e. if a study documents the results from testing multiple distinct nanoparticles, the study is subdivided to reflect the number of particles tested. For example, the third row of Table 1 refers to a single publication that included data for two nanoparticle variants, one silica nanoparticle, and one titanium dioxide nanoparticle. The dataset was analyzed for the 5 toxicological endpoints discussed earlier and their ideal cluster combinations were derived, each cluster is defined by a distinct dose-response-recovery model. The algorithm aligned the pulmonary effects of different MONP variants based on the similarity of their dose-response-recovery relationships. Fig. 2 is a comparison of the variation in AICc values for all 5 response indicators used in the study, it also serves to determine the ideal number of clusters for each indicator. The decrease in the AICc of the clusters at each stage observed in Fig. 2 is an indicator that the clustering process works (information retained increases as the number of clusters increases).

The decision on the ideal number of clusters that can be used to represent the MONP dataset is based on the trade-off between a penalty for increasing the number of toxicologically unique clusters (i.e. increasing model complexity) and the benefits of new information gleaned from them (i.e. reduced model error). Analyzing the variation in AICc documented in Fig. 2, a single consensus cluster size could not be agreed upon across the 5 responses for the MONPs due to the varying size of the number of particles analyzed for each response.

The clusters generated by the algorithm exist on the basis of similarity between their toxicological profiles but that does not fully explain

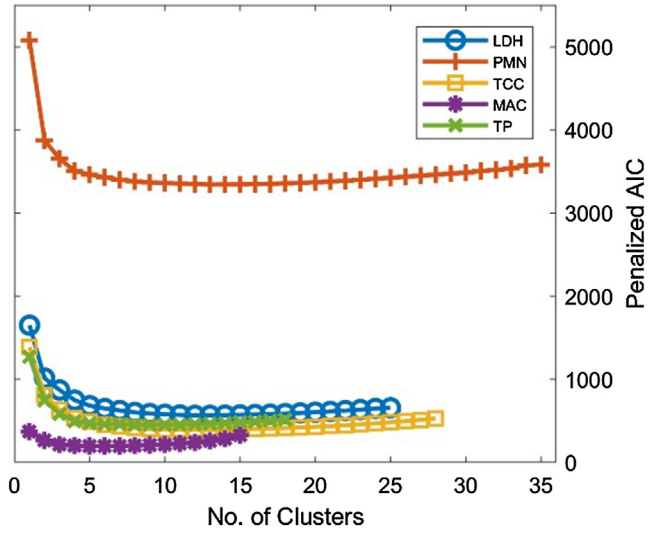

Fig. 2. Penalized Akaike Information Criterion (AICc) as a function of the number of clusters. The figure illustrates the variation in the number of particles analyzed for each response and hence the lack of a consensus optimum number across the 5 responses.

the existence of the clusters. To further investigate the clusters, we examine and study the particle variants within each of the clusters. Contrasting the physical and chemical characteristics of the different particle configurations could lead to the generation of hypotheses as to why one cluster or class of nanoparticles may be more or less toxic than another. The reasoning the MONP dataset constituents are not segregated initially based on their physical/chemical properties is that physically and/or chemically similar nanomaterials need not necessarily be similar in their dose-response-recovery relationships as well, depending on which characteristics are used to define similarity. Identifying the particle properties that do and do not vary significantly between the clusters assists in determining which properties are key contributors in the separation at each stage and also towards the relative toxicity between the clusters. Table 1 is an account of all the publications that have been used as data sources for the MONP. Table 1 also provides a comprehensive look at the information available to the authors during the process, namely the types of particles tested by each publication, the number of endpoints measured, and the physical characteristics reported. We can observe from Table 1, that not all the source publications report all 5 endpoints and some sources are also missing or lacking in sufficient physical characterization data. The disparity in endpoint measures reported by the source publications is one cause of cluster membership that is not consistent across the 5 endpoints.

The MONP groupings generated by the clustering process were examined to identify and highlight any trends between the clusters and their particle properties. The optimal number of clusters for the PMN, LDH and TCC responses was found to be 8 based on the AICc values, the MAC and TP endpoints had an optimal cluster quantity of 4. The lack of a consensus amongst the 5 endpoints analyzed could be associated with the number of particle variants analyzed for each endpoint. It can be observed from Fig. 2 that the 3 endpoints with a higher minimum cluster size also had larger number of particle variants with reported measurements from the BAL fluid. Table 2 displays the particle properties and membership composition of the MONP clusters for the PMN response. The "Particle Typical Size" measurement is the mean diameter for the spherical MONPs that were analyzed. There is no obvious trend between the primary particle size and the cluster composition for this particular response independent of particle composition. Analysis of the 4 other responses for the MONPs revealed the same. This could imply that creating category labels for the MONP clusters purely using either the physical properties and/or chemical composition might not be possible with the available data and a different approach might be required.

3.2. Results of clustering by particle composition

The initial clustering process treated each of the individual MONP variants analyzed from each study as a unique substance. This leads to instances of similar substances appearing in multiple clusters as

Table 2
Mean "typical particle size" for MONP clusters along with constituent cluster composition for PMN response. The composition of the clusters indicates that multiple metal oxide particles can be categorized together by virtue of their dose- response-recovery relationships.

Cluster	Mean Particle size (nm)	Cluster Composition
1	1228.4	Crystalline Silica, Amorphous Silica
2	3133.3	Titanium Dioxide, Alumina, Copper Oxide
3	14.6	Titanium Dioxide
4	232.8	TiO_2, NiO, Crystalline Silica, ZnO, CeO_2
5	107.7	TiO_2, Fe_2O_3
6	164.4	TiO_2, Amorphous Silica, ZnO
7	13.9	CeO_2, Crystalline Silica
8	154	TiO_2, Crystalline Silica, ZnO, CeO_2

Table 3
Fractional overlap of exposure group data between the measured endpoints from the BAL fluid of the animals.

Measured Endpoint	TCC	PMN	LDH	TP	MAC
TCC	1	0.70	0.61	0.58	0.37
PMN		1	0.73	0.55	0.29
LDH			1	0.59	0.25
TP				1	0.42
MAC					1

evidenced in Table 2. For example, crystalline silica nanoparticle variants appear in 4 of the 8 clusters. The information provided in Table 2 for the MONP clusters does not seem to provide evidence of any discernable pattern between the particle properties (such as size, or aggregation, or solubility, or bond strength) and membership for the respective clusters. The treatment of the particle variants from each study as unique entities results in a skewed distribution across the clusters, for example Titanium Dioxide (TiO_2) was the most commonly tested particle and appears in 6 out of the 8 clusters as seen in Table 2. To eliminate the multiple instances of the same substance occurring across the clusters in a secondary analysis, the particle variants were grouped in the dataset based on their chemical composition and the clustering process was repeated. The repeat of the clustering process post composition-grouping allows for different distinctions to be made between clusters.

Fig. 3 is a comparison of the AICc variation between chemically isolated particles across the 5 response indicators. The composition grouping process reduced the number of particle groups to between 7 and 9 per response. We can observe from the figure that the ideal number of clusters across the 5 responses is 4, implying that there are 4 toxicologically unique clusters amongst the different metal oxide particles. The choice of 4 clusters as the ideal set is based on weighing the value of additional information conveyed against the increasing complexity (> 5 clusters), the 4-cluster model provide the best balance between information conveyed and overall complexity. The clustering methodology employed was validated using a leave-one-out meta-analysis approach. 95% of the validation process iterations resulted in 4 clusters as the best solution and the remaining 5% of iterations had 4 clusters within 1 standard error of the minimum. The validation of the clustering process emphasizes the consistency of the algorithm and the

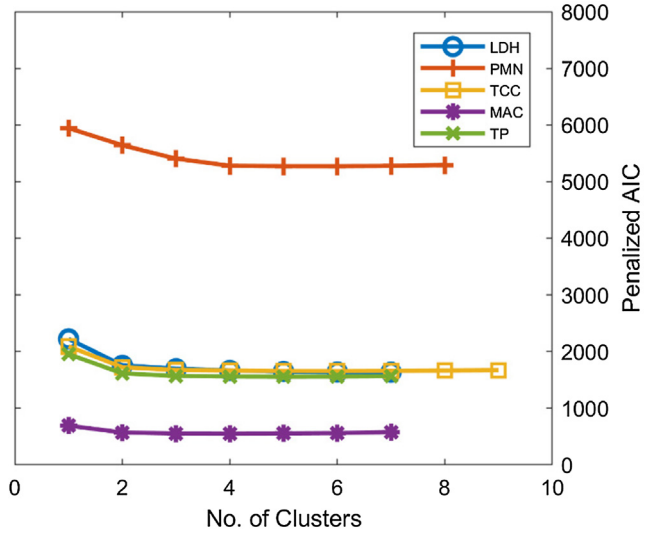

Fig. 3. Corrected Akaike Information Criterion (AICc) as a function of the number of clusters in the model. The figure illustrates the optimum number of clusters is 4 based on the minimum achieved for all endpoints indicating there are 4 distinct groups of MONPs.

Table 4
Clusters generated across the 5 endpoints for the various metal oxides (data sources are indicated in parentheses). The bolded elements illustrate particle composition "anchors" across the clustering results.

Cluster ID	LDH Clusters	TCC Clusters	MAC Clusters	PMN Clusters	TP Clusters
I	**Iron *(F2, F3, F5)***	**Iron *(F1, F2)***, Zinc ***(Z1, Z4-Z6)***, Cerium ***(Ce1, Ce2, Ce5, Ce6)***	Cerium ***(Ce1, Ce3, Ce5, Ce6)***	**Iron *(F2, F3, F5)***	**Iron *(F3)***
II	**Silica *(S1, S3-S6, S8, S10, S11, S14-S16)***	**Silica *(S1- S3, S5- S8, S10, S12, S14, S16, S18)***, Copper ***(Cu1, Cu2)***, Nickel ***(N2, N5-N8)***	**Silica *(S2, S6-S9, S13, S14, S16)***, Nickel ***(N1)***	**Silica *(S1, S3-S5, S7, S10-S12, S14, S16)***, Copper ***(Cu1, Cu2)***, Aluminum ***(A1)***	**Silica *(S1, S3, S4, S7-S9, S11, S13, S14, S16, S17)***, Cerium ***(Ce1, Ce2, Ce4)***
III	Zinc ***(Z1-Z3, Z6)***, Cerium ***(Ce1, Ce3, Ce4, Ce7-Ce9)***, Aluminum ***(A1)***	Aluminum ***(A1)***, Cobalt ***(Co1, Co2)***	Cobalt ***(Co1, Co2)***	Zinc ***(Z1–Z6)***, Cerium ***(Ce2, Ce3, Ce6, Ce8)***, Nickel ***(N2, N6)***	Zinc ***(Z3, Z4, Z6)***, Nickel ***(N2-N4)***
IV	**Titanium *(T3, T6–T9, T11, T12, T17, T19, T20)***, Magnesium ***(M1)***	**Titanium *(T2–T7, T9-T11, T13, T15, T17–T19, T22)***	**Titanium *(T1, T2, T5, T10, T12, T13, T16–T19)***, Iron ***(F2, F4)***, Aluminum ***(A1)***	**Titanium *(T1-T5, T7-T12, T14, T15, T17)***	**Titanium *(T3–T8, T16, T17, T19–T21)***, Aluminum ***(A1)***

Table 5
Potency values for response across cluster categories ($b \times 10^{-14}$). The disparity between the highest and lowest values for potency can be observed. The highest value is more than 400,000 times larger than the lowest across all the responses which further stresses the need for sub-groups.

Cluster ID	LDH	PMN	Total Protein	Macrophages	Total Cell Count
I	105	40.5	1060	313	1960
II	2.36E+06	102	553	30.4	464
III	6.67E+05	5.18	166	85	611
IV	1.08E+06	103	867	146	825

clusters generated. Tables 4 and 5 display the newly clustered metal oxide particle variants (that have been grouped chemically) and the associated potency of the respective clusters. It can be observed that there is a level of consistency to clustering process in Table 4 that was not visible before in Table 2. Table 3 illustrates the degree of consistence of the specific observations (dose-recovery groups with the same particle variant) amongst the 5 endpoints. We can see that most particle types were tested for more than one endpoint with the exception of those evaluated for changes in macrophage count.

As mentioned in Section 2.2 and Eq. (1), the recovery of an animal following the end of toxic exposure is expected to follow an exponential relationship as the subject returns to homeostasis. However, limitations in the available data set did not support the differentiation between this expected relationship and a linear model. In Fig. 4, one can observe the comparison between the linear and exponential models in the AIC results for each toxic endpoint modeled. These results are very similar with AIC values for the linear recovery model being either nearly equivalent or up to 5% lower than those of the exponential model. Given these results there is no positive statistical justification to use the more complex exponential model at this time, though future data collection may change this assessment.

3.2.1. Observed differences in toxicity

The potency values for the 5 responses reported in Table 5 displays the quantification of the relative differences in toxicity between the clusters. Higher values of potency reflect greater toxic potential for the set of nanoparticle variants in the cluster. Based on the values in Table 5 we can observe that there is a substantial difference between the potency of the particle variants for LDH. The variation between the

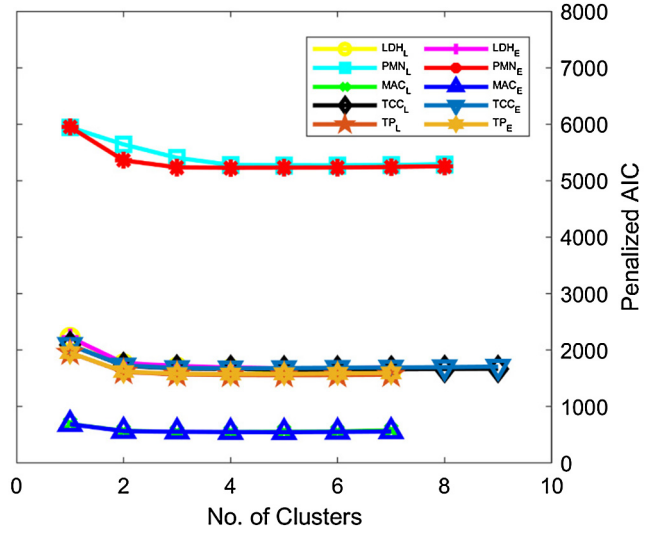

Fig. 4. Corrected Akaike Information Criterion (AICc) comparison between models with a linear recovery (L) versus models with an exponential recovery (E). The lack of any discernable difference between the AICc values is evidence to back our assumption of a linear recovery.

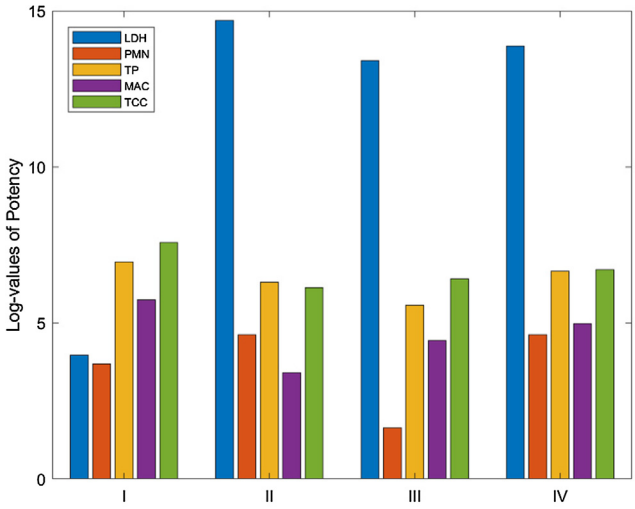

Fig. 5. The variation between natural logs of the potency of the responses in each cluster provides insight towards the observed effects each cluster of particles has on the response. LDH response levels were highly elevated for clusters 'II', 'III' and 'IV'.

potency of the particle variants and associated clusters supports the need for categories amongst metal oxide particles, and a significant limitation of treating them as the same substance in a risk assessment or regulatory framework (e.g., such as "ultrafine particulates"). The physical and chemical properties described in Table 1 for the metal oxide nanoparticle variants could potentially be utilized to derive characteristic-based definitions for the clusters. However, the lack of consistency in the endpoints reported by the source publications coupled with the skew in the particle variants tested (22 articles reported Titanium dioxide while only 5 reported Iron and 6 reported Zinc) leads to a low degree of consistency in the toxicological and particle characterization data across the clusters which precludes the possibility of deriving statistically significant property-based labels. A more consistent testing and reporting procedure would assist in identifying the mechanistic variations in toxicity due to physical characteristics and deriving labels for the clusters. Such recommendations have been published for nanoparticle characterization, but there has so far been limited programming of toxicological research regarding specific particle variants and dose levels [77–79].

Fig. 5 is a graphical presentation of the natural log of the potency across the clusters. Higher values for potency result in greater increase in the response for a unit increase in dose. For example, the high value of potency for the LDH response levels imply that for even small increases in nanoparticle dose the LDH levels in the subject would show significantly larger increases compared to the other 4 responses. LDH or Lactate Dehydrogenase is an enzyme and a core component of the energy production system in the body, it is involved in the conversion of "Nicotinamide adenine dinucleotide (NAD)" to its reduced form "NAD + Hydrogen (NADH)". LDH is not normally located outside cells. LDH appears outside cells in fluids like blood or BAL fluid when cell membranes are leaking or have been ruptured. Sharp changes in the LDH levels are usually associated with tissue damage. Identifying the clusters and particles which contribute to increased potency levels for the LDH could be useful in early detection and mitigation of tissue damage.

Fig. 6 compares the standardized potency of the clusters across the 5 responses, standardizing the potency makes it easier to compare the various response groups directly and determine their relative extent of threat. It can be seen in Fig. 6 that the particles belonging to clusters 'I', 'II' and 'IV' display signs associated with cell membrane damage and tissue damage/immune response. The cluster designated as 'III' is noteworthy as it is the only cluster that displays reduced response activity

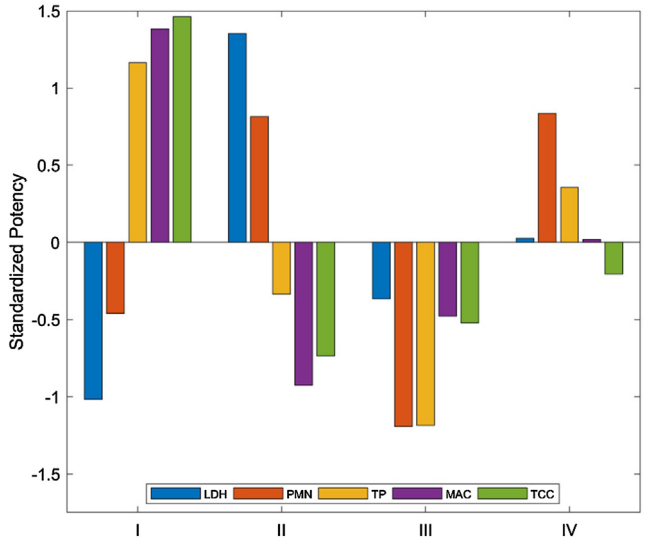

Fig. 6. The variation of the standardized potency of the responses across the clusters allows for easier interpretation of the observed effects of exposure to the particle clusters. Cluster 'I', 'II" and 'IV' shows signs of increased cell damage and elevated immune response. Cluster 'III' shows below average toxic potency across all 5 measured endpoints.

below the typical (i.e. mean) levels, this is indicative that the particles categorized as belonging to cluster 'III' possess less toxic potential than the particles in the other 3 clusters. Cluster 'III' is comprised primarily of Zinc oxide nanoparticles (3 out of 5 responses), previous literature has indicated that nano-Zinc oxide is non-toxic based on exposure studies conducted on mice [80]. Sayes et al. (2007) provided insight into the *in vivo* toxicity of nano-Zinc oxide and noted that acute toxicity response does exist, they were able to conclude that the effects were transient in nature and resolved themselves [30]. Nano-Zinc oxide is also highly commercialized and extensively used in sunscreen [81], a previous study was able to conclude that Zinc oxide nanoparticles greater than 30 nm in size exhibit the same properties as their non-nano counterparts [82]. While these results cannot conclusively assist in classifying Zinc oxide nanoparticles as non-toxic, they do offer some insight into the relatively low toxic potency of cluster 'III'.

Also, the normalized response indicator levels between clusters 'I' and 'II' are inverse to one another, cluster 'II' displays elevated LDH and PMN levels whereas cluster 'I' nanoparticles showed reduced LDH and PMN levels and vice versa with respect to the other 3 endpoints measured. Cluster 'I' is primarily rich in Iron nanoparticles, while cluster 'II' is mainly composed of Silica nanoparticles. Previous studies have compared the acute toxicity of Iron oxide and Silica nanoparticles, one study noted that no dose-related changes were observed in rats that were orally administered the nanoparticles [83]. Comparison of the individual cluster components across the 5 responses shows they differ in their chemical composition but more information is required before we hypothesize about the specific toxicological mechanism behind the differences in potency.

3.2.2. Possible policy implications

These results suggest that it may be possible and desirable to establish toxicological categories of engineered metal oxide nanoparticles and establish regulatory policy around those categories rather than seeking to establish a nano-specific exposure limit for each of the currently regulated solid particles. There are currently 10 of metal oxide particle exposure limits existing in OSHA regulations as of the date of this paper [84]. If regulatory agencies would follow the pattern of the NIOSH REL for titanium dioxide and establish exposure limits that vary with metal oxide particle size for each of these particles, the burden and cost of demonstrating compliance or non-compliance would be substantially increased. While this paper has not included ease of detection as a parameter for defining clusters, such an analysis could be conducted to develop categories that did account for this factor.

Beyond possible implications for defining exposure limits on a categorical rather than a specific-particle-by-specific-particle basis, these categories could also provide useful for the purposes of categorizing particular engineered nanoparticle variants for increased scrutiny as to their safety. Even in the absence of specific national regulations, new chemical products including engineered metal oxide nanoparticle products need to be approved for use. Those particles composed of constituents in the more toxic clusters should be prioritized for additional data gathering for safety purposes above those in the least toxic cluster. For example, based on these results, iron oxide, cerium oxide and silicon dioxide nanoparticles would be prioritized over zone, nickel, or aluminum oxide.

4. Conclusions

This analysis suggests that it is possible to define clusters or categories of metal oxide nanoparticles that behave similarly in terms of their dose-response-recovery effect on animals, which may be helpful in the future to maintain safety while also encouraging development of these materials without excessive burdens on future regulators. Further, this analysis indicates that 3 out of the 4 identified composition-based clusters display elevated response levels consistent with cellular damage (increased TP), onset of cytotoxicity (increased LDH) and immune activity (increased MAC, PMN and TCC). These are consistent with previously published literature on the toxicological effects of metal oxide nanoparticles.

This study demonstrates deployment of a hierarchical clustering algorithm to perform a meta-analysis of the *in vivo* pulmonary toxicity of engineered nanomaterials (specifically metal-oxide nanoparticles) in rodents. The argument for utilizing this algorithm over other available alternatives is the emphasis placed on the dose- response and recovery patterns rather than treating the available parameters as equivalent to particle properties, or assuming that all necessary physicochemical characteristics are already known. The process assists in generating hypotheses in regard to what mechanisms or characteristics might explain why certain particles cause similar or dissimilar pulmonary effects. The two iterations of the clustering on the MONP dataset produced 2 different set of results. The initial analysis treated the multiple MONPs analyzed as unique variations and performed the clustering leading to the identification of 8 toxicologically distinct clusters. There was a lack of relation between the characteristics of the MONP clusters and their composition, which limited the definitive description of the distinct clusters. The second iteration was performed after chemically grouping the various MONPs, the results were much more promising with 4 toxicologically distinct clusters being identified.

This work and the identified clusters propose that certain characteristics/nanoparticles are significant or insignificant to the identification of toxic potency. The clusters were further categorized into potential classes defined by their potency. The lack of sufficient characterization data does not prevent the use of this algorithm, although it may limit the definitive description (property-based labels) of the distinct clusters after the fact. Nanomaterials behaving in a similar/dissimilar pattern can be identified and grouped together and their differing attributes can be identified and related to their potency.

The analysis of the potency of the MONP clusters using the response variables was able to reveal that all but one group (cluster "III") of metal oxide particles have the potential to cause increased cell damage and immune response intensity due to their elevated levels for the response indicators analyzed. The toxicological behavior of the particles belonging cluster 'III' is worthy of further investigation to explore the underlying cause, it could be representative of certain particles in tandem displaying the capability to mitigate their respective biological effects. Overall, this study has shown that the potency of the

nanoparticle clusters might not depend just on the physical and/or chemical characteristics, expansion to include more properties to explain the relationship could be meaningful. These results could also be interpreted as a sign that a simple relationship between potency and the physical and/or chemical characteristics is either non-existent or that it is more complex than anticipated and requires further investigation.

5. Author information

Author contributions

The manuscript was written through contributions of all authors. All authors have given approval to the final version of the manuscript and contributed equally.

Declaration of Competing Interest

The authors declare that they have no known competing financial interests or personal relationships that could have appeared to influence the work reported in this paper.

Acknowledgments

Funding for this work was provided by NIOSH, through grant 1 R03 OH010956-01. This work has also been supported by the National Science Foundation (NSF) and the Environmental Protection Agency (EPA) under NSF Cooperative Agreement EF-0830093, Center for the Environmental Implications of NanoTechnology (CEINT).

References

[1] USEPA, Economic Analysis of the Proposed Change in Data Requirements Rule for Conventional Pesticides. US Environmental Protection Agency, 2004.
[2] A. Prabu, R.B. Anand, Emission control strategy by adding alumina and cerium oxide nano particle in biodiesel, J. Energy Inst. 89 (3) (2016) 366–372.
[3] A. Weir, et al., Titanium dioxide nanoparticles in food and personal care products, Environ. Sci. Technol. 46 (4) (2012) 2242–2250.
[4] J.Y.C. Ma, et al., Interactive effects of cerium oxide and diesel exhaust nanoparticles on inducing pulmonary fibrosis, Toxicol. Appl. Pharmacol. 278 (2) (2014) 135–147.
[5] L. Peng, et al., Comparative pulmonary toxicity of two ceria nanoparticles with the same primary size, Int. J. Mol. Sci. 15 (4) (2014) 6072–6085.
[6] A. Gustafsson, et al., Lung exposure of titanium dioxide nanoparticles induces innate immune activation and long-lasting lymphocyte response in the Dark Agouti rat, J. Immunotoxicol. 8 (2) (2011) 111–121.
[7] W.S. Cho, et al., Metal oxide nanoparticles induce unique inflammatory footprints in the lung: important implications for nanoparticle testing, Environ. Health Perspect. 118 (12) (2010) 1699–1706.
[8] W.S. Cho, et al., Progressive severe lung injury by zinc oxide nanoparticles; the role of Zn2+ dissolution inside lysosomes, Part. Fibre Toxicol. 8 (2011).
[9] R.M. Silva, et al., Biological response to nano-scale titanium dioxide (Tio2): role of particle dose, shape, and retention, J. Toxicol. Environ. Health-Part A-Current Issues 76 (16) (2013) 953–972.
[10] NIOSH, Occupational Exposure to Titanium Dioxide. National Institute for Occupational Safety and Health, 2011.
[11] A. Yassin, F. Yebesi, R. Tingle, Occupational exposure to crystalline silica dust in the United States, 1988–2003, Environ. Health Perspect. 113 (3) (2005) 255–260.
[12] J.Y. Choi, G. Ramachandran, M. Kandlikar, The impact of toxicity testing costs on nanomaterial regulation, Environ. Sci. Technol. 43 (9) (2009) 3030–3034.
[13] M.C. Roco, The long view of nanotechnology development: the National Nanotechnology Initiative at 10 years, J. Nanopart. Res. 13 (2) (2011) 427–445.
[14] T. Puzyn, et al., Using nano-QSAR to predict the cytotoxicity of metal oxide nanoparticles, Nat. Nanotechnol. 6 (3) (2011) 175–178.
[15] B. Rasulev, et al., Nano-QSAR: advances and challenges towards efficient designing of safe nanomaterials: innovative merge of computational approaches and experimental techniques, RSC Nanosci. Nanotechnol. 25 (2013) 220–256.
[16] N.G. Bakhtyari, et al., Prediction of genotoxicity of nano metal oxides by computational methods: a new decision tree QSAR model, Environ. Mol. Mutagen. 55 (2014) S43-S43.
[17] Y. Pan, et al., Nano-QSAR modeling for predicting the cytotoxicity of metal oxide nanoparticles using novel descriptors, RSC Adv. 6 (31) (2016) 25766–25775.
[18] R.S. Sexton, R.E. Dorsey, J.D. Johnson, Optimization of neural networks: a comparative analysis of the genetic algorithm and simulated annealing, Eur. J. Oper. Res. 114 (3) (1999) 589–601.
[19] J.M. Gernand, E.A. Casman, Machine learning for nanomaterial toxicity risk assessment, IEEE Intell. Syst. 29 (3) (2014) 84–88.
[20] J.M. Gernand, E.A. Casman, A meta-analysis of carbon nanotube pulmonary toxicity studies-how physical dimensions and impurities affect the toxicity of carbon nanotubes, Risk Anal. 34 (3) (2014) 583–597.
[21] X.H. Chang, et al., Health effects of exposure to nano-TiO2: a meta-analysis of experimental studies, Nanoscale Res. Lett. 8 (2013) 1–10.
[22] D.A. Notter, D.M. Mitrano, B. Nowack, Are nanosized or dissolved metals more toxic in the environment? A meta-analysis, Environ. Toxicol. Chem. 33 (12) (2014) 2733–2739.
[23] L.G. Hernández, et al., Can carcinogenic potency be predicted from in vivo genotoxicity data? A meta-analysis of historical data, Environ. Mol. Mutagen 52 (7) (2011) 518–528.
[24] J. Ioannidis, J. Lau, Pooling research results: benefits and limitations of meta-analysis, Joint Commission J. Quality Improvement 25 (9) (1999) 462–469.
[25] T.D. Spector, S.G. Thompson, The potential and limitations of meta-analysis, J. Epidemiol. Community Health 45 (2) (1991) 89.
[26] C. Kadoya, et al., Analysis of bronchoalveolar lavage fluid adhering to lung surfactant-experiment on intratracheal instillation of nickel oxide with different diameters, Ind. Health 50 (1) (2012) 31–36.
[27] M. Roursgaard, et al., Acute and subchronic airway inflammation after intratracheal instillation of quartz and titanium dioxide agglomerates in mice, Sci. World J. 11 (2011) 801–825.
[28] T. Oyabu, et al., Dose-dependent pulmonary response of well-dispersed titanium dioxide nanoparticles following intratracheal instillation, J. Nanopart. Res. 15 (4) (2013).
[29] G. Oberdorster, et al., Role of the alveolar macrophage in lung injury: studies with ultrafine particles, Environ. Health Perspect. 97 (1992) 193–199.
[30] C.M. Sayes, K.L. Reed, D.B. Warheit, Assessing toxicity of fine and nanoparticles: comparing in vitro measurements to in vivo pulmonary toxicity profiles, Toxicol. Sci. 97 (1) (2007) 163–180.
[31] O. Creutzenberg, et al., Toxicity of a quartz with occluded surfaces in a 90-day intratracheal instillation study in rats, Inhalation Toxicol. 20 (11) (2008) 995–1008.
[32] V.H. Grassian, et al., Inflammatory response of mice to manufactured titanium dioxide nanoparticles: comparison of size effects through different exposure routes, Nanotoxicology 1 (3) (2007) 211–226.
[33] R.C. Lindenschmidt, et al., The comparison of a fibrogenic and 2 nonfibrogenic dusts by bronchoalveolar lavage, Toxicol. Appl. Pharmacol. 102 (2) (1990) 268–281.
[34] M. Roursgaard, et al., Time-response relationship of nano and micro particle induced lung inflammation. Quartz as reference compound, Hum. Exp. Toxicol. 29 (11) (2010) 915–933.
[35] D.B. Warheit, et al., Pulmonary exposures to Sepiolite nanoclay particulates in rats: resolution following multinucleate giant cell formation, Toxicol. Lett. 192 (3) (2010) 286–293.
[36] D.B. Warheit, C.M. Sayes, K.L. Reed, Nanoscale and fine zinc oxide particles: can in vitro assays accurately forecast lung hazards following inhalation exposures? Environ. Sci. Technol. 43 (20) (2009) 7939–7945.
[37] M. Ban, et al., Effect of submicron and nano-iron oxide particles on pulmonary immunity in mice, Toxicol. Lett. 210 (3) (2012) 267–275.
[38] W.S. Cho, et al., Differential pro-inflammatory effects of metal oxide nanoparticles and their soluble ions in vitro and in vivo; zinc and copper nanoparticles, but not their ions, recruit eosinophils to the lungs, Nanotoxicology 6 (1) (2012) 22–35.
[39] B. Katsnelson, et al., Some peculiarities of pulmonary clearance mechanisms in rats after intratracheal instillation of magnetite (Fe3O4) suspensions with different particle sizes in the nanometer and micrometer ranges: are we defenseless against nanoparticles? Int. J. Occup. Environ. Health 16 (4) (2010) 508–524.
[40] M.T. Zhu, et al., Comparative study of pulmonary responses to nano- and submicron-sized ferric oxide in rats, Toxicology 247 (2–3) (2008) 102–111.
[41] K. Gelli, M. Porika, R.N.R. Anreddy, Assessment of pulmonary toxicity of MgO nanoparticles in rats, Environ. Toxicol. 30 (3) (2015) 308–314.
[42] T.A. Xia, et al., Decreased dissolution of ZnO by Iron doping yields nanoparticles with reduced toxicity in the rodent lung and Zebrafish embryos, ACS Nano 5 (2) (2011) 1223–1235.
[43] D. Fourches, D.Q.Y. Pu, A. Tropsha, Exploring quantitative nanostructure-activity relationships (QNAR) modeling as a tool for predicting biological effects of manufactured nanoparticles, Comb. Chem. High Throughput Screening 14 (3) (2011) 217–225.
[44] C. Sayes, I. Ivanov, Comparative study of predictive computational models for nanoparticle-induced cytotoxicity, Risk Anal. 30 (11) (2010) 1723–1734.
[45] R. Liu, et al., Classification NanoSAR development for cytotoxicity of metal oxide nanoparticles, Small 7 (8) (2011) 1118–1126.
[46] D. Fourches, et al., Quantitative nanostructure-activity relationship modeling, ACS Nano 4 (10) (2010) 5703–5712.
[47] S. Kang, M.S. Mauter, M. Elimelech, Physicochemical determinants of multiwalled carbon nanotube bacterial cytotoxicity, Environ. Sci. Technol. 42 (19) (2008) 7528–7534.
[48] V. Ramchandran, J.M. Gernand, A dose-response-recovery clustering algorithm for categorizing carbon nanotube variants into toxicologically distinct groups, Comput. Toxicol. 11 (2019) 25–32.
[49] A.H. Halim, I. Ismail, Combinatorial optimization: comparison of heuristic algorithms in travelling salesman problem, Arch. Comput. Methods Eng. 26 (2) (2019) 367–380.
[50] Inc., T.M., MATLAB R2017b. Natick, MA, USA.
[51] A. Adewole, et al., A comparative study of simulated annealing and genetic algorithm for solving the travelling salesman problem, Int. J. Appl. Inf. Syst. (IJAIS) 4 (4) (2012) 6–12.
[52] M. Andresen, et al., Simulated annealing and genetic algorithms for minimizing

mean flow time in an open shop, Math. Comput. Modell. 48 (7–8) (2008) 1279–1293.
[53] A. Kerr, K. Mullen, A comparison of genetic algorithms and simulated annealing in maximizing the thermal conductance of harmonic lattices, Comput. Mater. Sci. 157 (2019) 31–36.
[54] A. Nemmar, K. Melghit, B.H. Ali, The acute proinflammatory and prothrombotic effects of pulmonary exposure to rutile TiO2 nanorods in rats, Exp. Biol. Med. (Maywood) 233 (5) (2008) 610–619.
[55] D.B. Warheit, et al., Pulmonary instillation studies with nanoscale TiO2 rods and dots in rats: toxicity is not dependent upon particle size and surface area, Toxicol. Sci. 91 (1) (2006) 227–236.
[56] L.C. Renwick, et al., Increased inflammation and altered macrophage chemotactic responses caused by two ultrafine particle types, Occup. Environ. Med. 61 (5) (2004) 442–447.
[57] B. Rehn, et al., Investigations on the inflammatory and genotoxic lung effects of two types of titanium dioxide: untreated and surface treated, Toxicol. Appl. Pharmacol. 189 (2) (2003) 84–95.
[58] D.B. Warheit, et al., Pulmonary toxicity study in rats with three forms of ultrafine-TiO2 particles: differential responses related to surface properties, Toxicology 230 (1) (2007) 90–104.
[59] N. Kobayashi, et al., Comparative pulmonary toxicity study of nano-TiO2 particles of different sizes and agglomerations in rats: different short- and long-term post-instillation results, Toxicology 264 (1–2) (2009) 110–118.
[60] J.R. Roberts, et al., Toxicological evaluation of lung responses after intratracheal exposure to non-dispersed titanium dioxide nanorods, J. Toxicol. Environ. Health-Part A-Curr. Issues 74 (12) (2011) 790–810.
[61] I. Gosens, et al., Impact of agglomeration state of nano- and submicron sized gold particles on pulmonary inflammation, Part. Fibre Toxicol. 7 (2010).
[62] W.S. Cho, et al., Inflammatory mediators induced by intratracheal instillation of ultrafine amorphous silica particles, Toxicol. Lett. 175 (1–3) (2007) 24–33.
[63] Y. Morimoto, et al., Inflammogenic effect of well-characterized fullerenes in inhalation and intratracheal instillation studies, Part. Fibre Toxicol. 7 (2010).
[64] S. Pirela, et al., Effects of copy center particles on the lungs: a toxicological characterization using a Balb/c mouse model, Inhalation Toxicol. 25 (9) (2013) 498–508.
[65] T. Toya, et al., Pulmonary toxicity induced by intratracheal instillation of coarse and fine particles of cerium dioxide in male rats, Ind. Health 48 (1) (2010) 3–11.
[66] Y. Morimoto, et al., Expression of inflammation-related cytokines following intratracheal instillation of nickel oxide nanoparticles, Nanotoxicology 4 (2) (2010) 161–176.
[67] J.Y. Ma, et al., Cerium oxide nanoparticle-induced pulmonary inflammation and alveolar macrophage functional change in rats, Nanotoxicology 5 (3) (2011) 312–325.
[68] E.J. Park, et al., Induction of inflammatory responses in mice treated with cerium oxide nanoparticles by intratracheal instillation, J. Health Sci. 56 (4) (2010) 387–396.
[69] C.J. Wingard, et al., Mast cells contribute to altered vascular reactivity and ischemia-reperfusion injury following cerium oxide nanoparticle instillation, Nanotoxicology 5 (4) (2011) 531–545.
[70] L.X. Xue, et al., Pulmonary toxicity of ceria nanoparticles in mice after intratracheal instillation, J. Nanosci. Nanotechnol. 13 (10) (2013) 6575–6580.
[71] V.C. Minarchick, et al., Pulmonary cerium dioxide nanoparticle exposure differentially impairs coronary and mesenteric arteriolar reactivity, Cardiovasc. Toxicol. 13 (4) (2013) 323–337.
[72] C.A.J. Dick, et al., The role of free radicals in the toxic and inflammatory effects of four different ultrafine particle types, Inhalation Toxicol. 15 (1) (2003) 39–52.
[73] Q.W. Zhang, et al., Differences in the extent of inflammation caused by intratracheal exposure to three ultrafine metals: role of free radicals, J. Toxicol. Environ. Health-Part A-Curr. Issues 53 (6) (1998) 423–438.
[74] M. Horie, et al., Comparison of acute oxidative stress on rat lung induced by nano and fine-scale, soluble and insoluble metal oxide particles: NiO and TiO2, Inhalation Toxicol. 24 (7) (2012) 391–400.
[75] A. Ogami, et al., Pathological features of different sizes of nickel oxide following intratracheal instillation in rats, Inhalation Toxicol. 21 (8–11) (2009) 812–818.
[76] K. Nishi, et al., Expression of cytokine-induced neutrophil chemoattractant in rat lungs by intratracheal instillation of nickel oxide nanoparticles, Inhalation Toxicol. 21 (12) (2009) 1030–1039.
[77] E.J. Cho, et al., Nanoparticle characterization: state of the art, challenges, and emerging technologies, Mol. Pharm. 10 (6) (2013) 2093–2110.
[78] J.K. Jiang, G. Oberdorster, P. Biswas, Characterization of size, surface charge, and agglomeration state of nanoparticle dispersions for toxicological studies, J. Nanopart. Res. 11 (1) (2009) 77–89.
[79] M. Hassellov, et al., Nanoparticle analysis and characterization methodologies in environmental risk assessment of engineered nanoparticles, Ecotoxicology 17 (5) (2008) 344–361.
[80] B. Wang, et al., Acute toxicological impact of nano- and submicro-scaled zinc oxide powder on healthy adult mice, J. Nanopart. Res. 10 (2) (2008) 263–276.
[81] T.G. Smijs, S. Pavel, Titanium dioxide and zinc oxide nanoparticles in sunscreens: focus on their safety and effectiveness, Nanotechnol. Sci. Appl. 4 (2011) 95–112.
[82] M. Auffan, et al., Towards a definition of inorganic nanoparticles from an environmental, health and safety perspective, Nat. Nanotechnol. 4 (10) (2009) 634–641.
[83] J.W. Yun, et al., Comparative toxicity of silicon dioxide, silver and iron oxide nanoparticles after repeated oral administration to rats, J. Appl. Toxicol. 35 (6) (2015) 681–693.
[84] (OSHA), O.S.H.A., TABLE Z-1 Limits for Air Contaminants. Toxic and Hazardous Substances. Occupational Safety and Health Standards.